



## Original Article

# Photocatalytic activity of undoped and sulfur-doped TiO<sub>2</sub> films grown by MOCVD for water treatment under visible light

Rodrigo T. Bento, Olandir V. Correa, Marina F. Pillis\*

Nuclear and Energy Research Institute, IPEN-CNEN/SP, University of São Paulo, Prof. Lineu Prestes Avenue 2242, Brazil



## ARTICLE INFO

## Keywords:

Titanium dioxide  
Ceramic coatings  
Sulfur-doped TiO<sub>2</sub> films  
Dye degradation  
H<sub>2</sub>S  
MOCVD

## ABSTRACT

Titanium dioxide ceramic coatings have been used as catalysts in green technologies for water treatment. However, without the presence of a dopant, its photocatalytic activity is limited to the ultraviolet radiation region. The photocatalytic activity and the structural characteristics of undoped and sulfur-doped TiO<sub>2</sub> films grown at 400 °C by metallorganic chemical vapor deposition (MOCVD) were studied. The photocatalytic behavior of the films was evaluated by methyl orange dye degradation under visible light. The results suggested the substitution of Ti<sup>4+</sup> cations by S<sup>6+</sup> ions into TiO<sub>2</sub> structure of the doped samples. SO<sub>4</sub><sup>2-</sup> groups were observed on the surface. S-TiO<sub>2</sub> film exhibited good photocatalytic activity under visible light irradiation, and the luminous intensity strongly influences the photocatalytic behavior of the S-TiO<sub>2</sub> films. The results supported the idea that the sulfur-doped TiO<sub>2</sub> films grown by MOCVD may be promising catalysts for water treatment under sunlight or visible light bulbs.

## 1. Introduction

Chemical species as dyes, pigments, antibiotics, pharmaceuticals and personal care products, disposed in the in the wastewater can cause serious problems to the environment and to human health [1,2]. The conventional water treatments are often not capable of eliminating such substances. Thus more effective methods have been proposed in order to promote the removal of industrial waste efficiently [3–5]. Heterogeneous photocatalysis is a green method that use the solar light as radiation source to activate a catalyst. The pollutants are completely mineralized during the treatment, avoiding the production of new waste. This is an oxidative process based on the generation of hydroxyl radicals (OH<sup>•</sup>), responsible for the contaminant degradation [6,7], and originated when a semiconductor material is irradiated with photon energy equal or greater than its band gap energy (E<sub>g</sub>) [5,8]. In recent years, among many semiconductors, titanium dioxide (TiO<sub>2</sub>) ceramic coatings have been successfully applied in photocatalytic processes for water treatment [9,10].

TiO<sub>2</sub> presents chemical and biological stability, antibacterial properties, non-toxicity, biocompatibility, corrosion resistance in many media and low price [11–13]. Among the advantages of employing TiO<sub>2</sub> films in heterogeneous photocatalysis, when compared to catalysts powders, there is the possibility of reusing the catalytic materials - an important requirement for practical applications of photocatalysis in

water treatment [14]. TiO<sub>2</sub> films can be obtained by several techniques, and present different structural properties and morphological characteristics depending on factors such as film thickness, precursor, grain size, growth temperature, and substrate [10]. Metallorganic chemical vapor deposition (MOCVD) is a process to grow films that uses organometallic compounds as precursors. The structural properties of the films obtained by MOCVD are determined by the deposition parameters and the chemical organometallic precursors used [10,15]. This is an attractive method, since it provides a good control of stoichiometry and thickness of the films, and uniformity of deposition [1,16].

Recent studies demonstrated that the anatase-TiO<sub>2</sub> is the crystalline phase with the highest catalytic activity, due to the high electron mobility, and high surface area [3,16–18]. However, without the presence of a dopant, the photocatalytic activity of anatase-TiO<sub>2</sub> is limited to the ultraviolet radiation region.

Modifications of the TiO<sub>2</sub> have been proposed in order to increase its use in photocatalysis [13,19]. Among the proposed strategies, the catalyst doping with metals and non-metals elements aims to reduce the E<sub>g</sub> of the catalyst and turns it active under visible light – which corresponds to 45% of the total energy of solar radiation [20]. Non-metal doping methods using elements such as sulfur have shown great potential for photocatalytic applications. Bayati, Moshfegh and Golestani-Fard [21] studied the synthesis of sulfur-doped TiO<sub>2</sub>. The authors observed that S<sup>4+</sup> and S<sup>6+</sup> ions replace Ti<sup>4+</sup> into the TiO<sub>2</sub> lattice. The

\* Corresponding author.

E-mail address: [mfpilllis@ipen.br](mailto:mfpilllis@ipen.br) (M.F. Pillis).<https://doi.org/10.1016/j.jeurceramsoc.2019.02.046>

Received 9 December 2018; Received in revised form 20 February 2019; Accepted 23 February 2019

Available online 25 February 2019

0955-2219/ © 2019 Elsevier Ltd. All rights reserved.

absorption edge of doped films shifts to significantly larger wavelengths when compared to undoped TiO<sub>2</sub>. Ohno et al. [22] and Han et al. [23] observed that S<sup>6+</sup> cation-doped TiO<sub>2</sub> absorbed visible light more strongly than the S<sup>2-</sup> anion-doped catalysts. Wang et al. [24] reported that the S-doped TiO<sub>2</sub> catalysts obtained by low-temperature hydrothermal oxidation of titanium disulfide (TiS<sub>2</sub>) can narrow the TiO<sub>2</sub> band gap, and improve the photocatalytic behavior when compared to S-TiO<sub>2</sub> obtained at high temperature.

Several experimental studies have been demonstrated the efficient use of hydrogen sulfide (H<sub>2</sub>S) gas as precursor to produce sulfur-doped TiO<sub>2</sub> catalysts [25–27]. In our previous studies [14], TiO<sub>2</sub> thin films were heated in a mixture of H<sub>2</sub>-2v.% H<sub>2</sub>S at 50 °C, 100 °C and 150 °C. The S-TiO<sub>2</sub> film doped at 50 °C presented the higher photocatalytic activity under visible light. According to some authors, the decomposition and adsorption of H<sub>2</sub>S on the TiO<sub>2</sub> surface occurs spontaneously in the presence of OH<sup>•</sup> radicals [28]. It has also been observed that the sulfur can be oxidized and adsorbed in the form of SO<sub>4</sub><sup>2-</sup> groups on the surface [27,28], and create Ti–O–S bonds into TiO<sub>2</sub> lattice [14,24,25].

S-TiO<sub>2</sub> films can be synthesized at low temperatures in a process similar to that used for the desulfurization of H<sub>2</sub>S over TiO<sub>2</sub> catalyst [29–31]. The desulfurization is conducted in temperatures between 20 and 80 °C and results in the deposition of SO<sub>4</sub><sup>2-</sup> groups on the surface of the TiO<sub>2</sub> [29,32]. Generally these catalysts are synthesized by the sol-gel method, and their application for water treatment is little explored. Furthermore, according to the literature TiO<sub>2</sub> films are usually sulfur-doped at temperatures above 300 °C [23,27,33].

In this way, sulfur-doped TiO<sub>2</sub> films obtained by a low-temperature alternative route were investigated in the present work. The doping was performed by using a process similar to that used for the desulfurization. The TiO<sub>2</sub> films were grown by MOCVD technique and then sulfur-doped at 50 °C in H<sub>2</sub>/H<sub>2</sub>S atmosphere. The photocatalytic behavior of the catalysts on the methyl orange dye degradation under visible light was evaluated, besides the structural and morphological characteristics of the films.

## 2. Experimental

### 2.1. Synthesis of TiO<sub>2</sub> films

TiO<sub>2</sub> thin films were grown by MOCVD process in a conventional horizontal reactor previously described by Bento et al. [10]. The growth of the films was carried out on borosilicate substrates (25 × 76 × 1 mm) previously cleaned in a 5% H<sub>2</sub>SO<sub>4</sub> aqueous solution, rinsed in deionized water, dried in nitrogen, and immediately inserted into the reactor. The films were grown at 400 °C under a pressure of 50 mbar. Titanium (IV) isopropoxide Ti[OCH(CH<sub>3</sub>)<sub>2</sub>]<sub>4</sub> (TTiP) (purity 99,999%, Sigma-Aldrich Co.) was used as the titanium and oxygen sources. N<sub>2</sub> was used as the carrier and the purge gas. The temperature of the bubbler containing TTiP was maintained at 39 °C. The flow rates of TTiP and N<sub>2</sub> were both fixed at 0.5 slm. The gas conduction lines are made of stainless steel and are kept heated to prevent condensation and premature pyrolysis of the precursor.

### 2.2. Sulfur-doped TiO<sub>2</sub> films

S-TiO<sub>2</sub> films were obtained by a thermochemical treatment realized in a horizontal tubular furnace at 50 °C for 60 min under a mixture of H<sub>2</sub>-2v.% H<sub>2</sub>S, with a flux of 0.2 slm. Heating and cooling to room temperature were performed under argon inert atmosphere.

### 2.3. Characterization of undoped and sulfur-doped TiO<sub>2</sub> films

X-ray diffraction (XRD) analyses were carried out in a Rigaku Multiflex equipment with a monochromatized CuKα radiation (λ = 1.54148 Å), incidence angle of 5°, scan rate of 0.02°, and with 2θ

ranging from 5 to 80°. The phases formed were identified with the JCPDS (Joint Committee on Powder Diffraction Standards) database. Surface roughness and mean grain size measurements were analyzed by atomic force microscopy (AFM) on the tapping mode (SPM Bruker NanoScope IIIA), employing a silicon tip with a curvature radius of 15 nm. The scan frequency used was 0.9 Hz and in the area of 5 μm × 5 μm. Mean grain size analyses were performed using the ImageJ<sup>®</sup> image processing software. X-ray photoelectron spectroscopy (XPS) was carried out in a Thermo Scientific K-Alpha equipment, with resolution of 0.1 eV, and spot size beam of 400 μm, in order to determine the chemical state of the species near the solid surface. Survey scans were collected over the 0–1200 eV binding energies range. Higher resolution scans encompassing the principal peaks of Ti 2p, O 1s and S 2p were collected at a pass energy of 50 eV. Chemical deconvolution was done using CasaXPS software [34], with the binding energies calibrated considering the C1s reference peak at 284.8 eV. Films thicknesses were measured on the cross-section of the samples using field emission scanning electron microscopy (FE-SEM) on JSM6701 F equipment.

### 2.4. Photocatalytic experiments

The photocatalytic activities of the films in the dye degradation were investigated in a homemade reactor setup previously described by Bento and Pillis [35]. The photoreactor consists of a glass chamber containing 40 mL of the dye solution (pH = 2) to be degraded, the catalyst that was supported on borosilicate substrate, and the radiation source. TiO<sub>2</sub> and S-TiO<sub>2</sub> films were used as catalysts and methyl orange (MO) dye as the model pollutant (0.005 g.L<sup>-1</sup>). Studies suggest that TiO<sub>2</sub> catalysts exhibit better photocatalytic activity under acidic solutions [14,16]. For the visible light tests, lamps of different intensities were employed to evaluate the influence of the light intensity on the photocatalytic behavior of the films. Firstly, a LED board (30 W; λ = 450 nm) was used as visible light source and, posteriorly, four tubular LED lamps (Royal Philips Electronics; 240 W; λ = 400–700 nm) were employed as radiation source. The lamps had a luminous flux of approximately 1300 lm (30 W) and 12,000 lm (240 W), so the luminous efficiency of these lamps was, respectively, 43.3 lm.W<sup>-1</sup> and 50 lm.W<sup>-1</sup>.

The dye degradation experiments were realized for a total test time of 300 min. The components of the photoreactor were arranged in a box to prevent loss of photons and to protect users against the emitted radiation. The distance between the catalyst and the radiation source was set at 250 mm. Synthetic air (N<sub>2</sub> / 20 wt.% O<sub>2</sub>) was bubbled into the solution during the tests. The experiments were kept under controlled temperature in the range of 19–20 °C. The system was kept under bubbling for one hour in the dark for allow the adsorption-desorption equilibrium of the solution on the catalyst. The MO dye concentration changes were examined using a UV–vis spectrophotometer (Global Trade Technology). During the photocatalytic experiments, the absorbance and pH values of the dye solution were constantly monitored every 30 min. After the measurement, the aliquots were returned to the solution.

## 3. Results and discussion

### 3.1. Structural and chemical characterization of undoped and sulfur-doped TiO<sub>2</sub> films

The crystallinity and phases formed in the grown films were investigated by XRD. Fig. 1 shows XRD patterns of the undoped and sulfur-doped TiO<sub>2</sub> films grown at 400 °C by MOCVD. From XRD results the films exhibit a good crystallinity constituted of peaks corresponding to 2θ angles of 25.3°, 48.1°, 55.1°, 62.7°, and 70.3°, respectively equivalent to the crystallographic planes (101), (200), (211), (204), and (220) [36]. These are characteristic peaks correspondent to the anatase

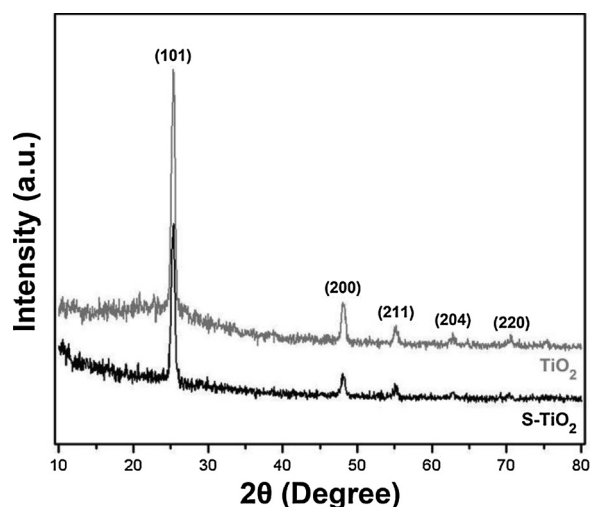


Fig. 1. XRD patterns of the undoped and sulfur-doped  $\text{TiO}_2$  films grown on borosilicate substrates at  $400^\circ\text{C}$  by MOCVD process.

crystalline phase (JCPDS 21-1272). The results suggest that the doping process did not alter the crystalline phase of  $\text{TiO}_2$  films, which agrees with results shown in the literature [25,37,38].

XPS measurements were realized to confirm the chemical elemental composition of the grown films. Fig. 2a compare the XPS survey spectrum of undoped and sulfur-doped  $\text{TiO}_2$  films. The presence of C 1s peak at 284.8 eV was ascribed to the residual carbon from the precursor, and to the adventitious carbon provoked by the sample exposition to air before the XPS experiments [35,38]. The survey spectra of S- $\text{TiO}_2$  revealed the presence of an additional peak of sulfur, denoting the successful inclusion of sulfur in  $\text{TiO}_2$ , with a sulfur concentration of 8.78 at% (Table 1). The surface of the films contains high quantities of Ti and O elements. Surface XPS analysis of the Ti 2p peaks for undoped  $\text{TiO}_2$  film (Fig. 2b) revealed binding energies at 459.5 eV and 465.3 eV attributed, respectively, to the Ti  $2p_{3/2}$  peak [36] – which corresponds to  $\text{Ti}^{4+}$  in  $\text{TiO}_2$  lattice [15,39] – and Ti  $2p_{1/2}$  peak [35,40], with a peak-to-peak separation of 5.8 eV, according with the reported values of  $\text{TiO}_2$

Table 1

Element analyses of undoped and sulfur-doped  $\text{TiO}_2$  films grown at  $400^\circ\text{C}$ .

	Ti (at%)	O (at%)	C (at%)	S (at%)	Total (at%)
undoped $\text{TiO}_2$	25.41	54.85	19.74	–	100
S- $\text{TiO}_2$	20.35	53.61	17.26	8.78	100

[41]. For S- $\text{TiO}_2$  film, (Fig. 2c) the binding energy peaks of Ti  $2p_{3/2}$  and Ti  $2p_{1/2}$  were found at 459.4 eV and 465.1 eV, respectively. The lower energy titanium peak values at 457.3 eV and 459.9 eV for undoped catalyst (Fig. 2b), and 457.1 eV and 459.5 eV for S- $\text{TiO}_2$  (Fig. 2c) confirmed the contribution of  $\text{Ti}^{3+}$  [38,40], and suggests the formation of Ti-O-S bonds [33]. It can be observed a slight displacement of the peaks. This result is in accordance with the literature. Such behavior was attributed to the oxygen vacancies or defects formed by substitutional sulfur into the  $\text{TiO}_2$  lattice [14,39,42].

Fig. 2d-e shows the O 1s XPS spectra of undoped and sulfur-doped  $\text{TiO}_2$  films. It can be observed a well-defined peak located at 530.7 eV for  $\text{TiO}_2$ , and 530.6 eV for S- $\text{TiO}_2$ , corresponding to oxygen in  $\text{TiO}_2$  lattice (Ti–O–Ti) [15,40], and a small shoulder peak centered at 532.4 eV and 532.2 eV for undoped and S- $\text{TiO}_2$ , respectively, which can be regarded as the  $\text{OH}^-$  adsorbed on the  $\text{TiO}_2$  surface [13,14].

The high-resolution XPS spectra for the S 2p region (Fig. 2f) exhibited the binding energy at 169.7 eV. According to previous studies [43], the peak observed from the fitted curve could correspond to sulfur on the higher oxidation state – commonly found in binding energy values above 168 eV. From the results sulfur species were identified as  $\text{S}^{6+}$  ions possibly replacing the  $\text{Ti}^{4+}$  ions into  $\text{TiO}_2$  structure, and also forming  $\text{SO}_4^{2-}$  sulfate groups on the surface [14,23,39]. The substitution effect is chemically more favorable for photocatalysis application than replacing  $\text{O}^{2-}$  by  $\text{S}^{2-}$ . The incorporation of  $\text{S}^{6+}$  cation in  $\text{TiO}_2$  structure can form an impurity energy level above the valence band, and reduce the  $\text{TiO}_2$  band gap to visible light radiation [42,44]. No indication of  $\text{S}^{2-}$  formation was observed at 161 eV, suggesting that it does not exist on the catalyst surface.

The mechanism of  $\text{H}_2\text{S}$  adsorption on the  $\text{TiO}_2$  surface can be described as dissociative pathways. The water molecules adsorbed on the  $\text{TiO}_2$  surface dissociate into  $\text{OH}^-$  and  $\text{H}^+$  ions [28,45]. The  $\text{OH}^-$

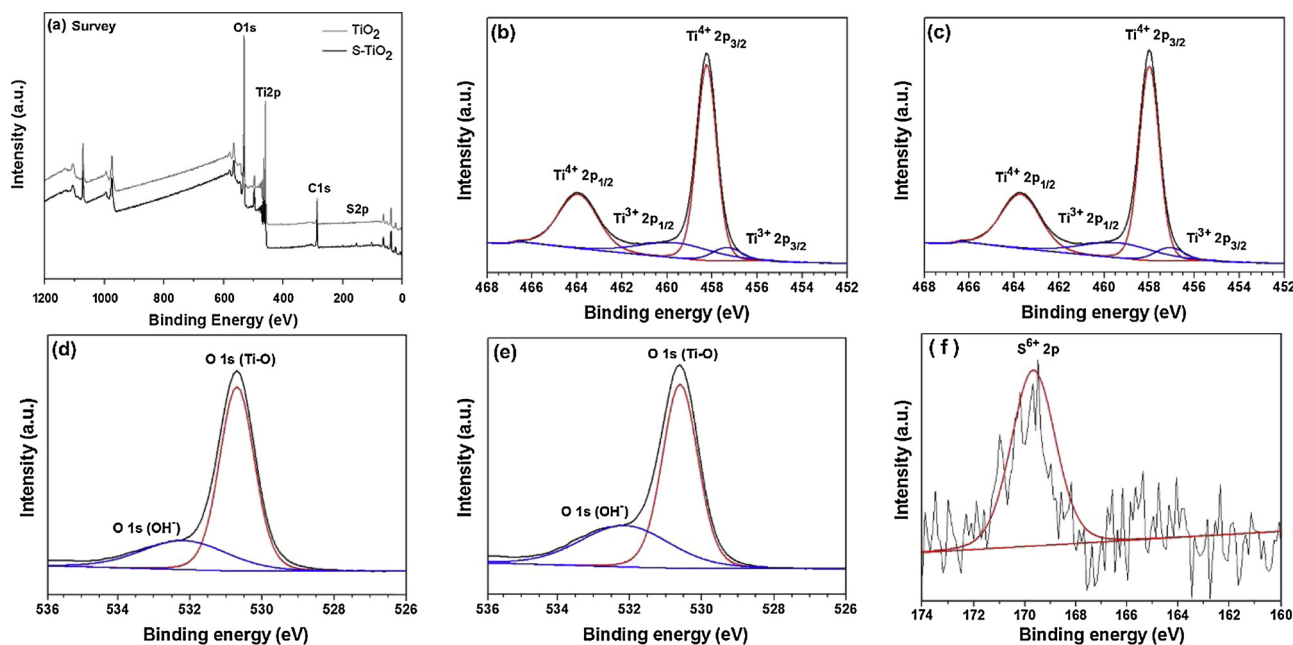


Fig. 2. (a) Survey XPS spectra of the undoped and sulfur-doped  $\text{TiO}_2$  films grown at  $400^\circ\text{C}$  by MOCVD. High resolution spectra XPS of: Ti 2p region with the fitted curves for (b) undoped and (c) sulfur-doped catalyst; O 1s region with the fitted curves for (d) undoped and (e) sulfur-doped catalyst; and (f) S 2p region with the fitted curves of sulfur-doped catalyst.

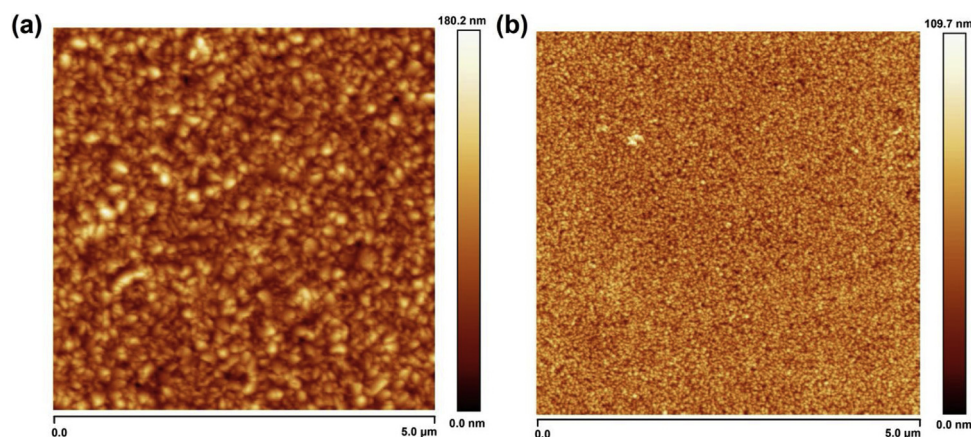
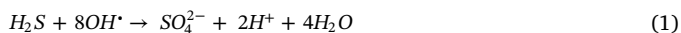


Fig. 3. AFM images of TiO<sub>2</sub> film grown at 400 °C on borosilicate substrate by MOCVD: (a) undoped and (b) sulfur-doped catalyst.

radicals are formed during the thermal treatment when OH<sup>-</sup> surface groups donate an electron (e<sup>-</sup>) to the hole (h<sup>+</sup>) [45,46]. Then, the presence of SO<sub>4</sub><sup>2-</sup> species on the catalyst surface may be explained by the oxidation reaction between H<sub>2</sub>S and the abundant OH<sup>·</sup> radicals formed on the TiO<sub>2</sub> surface, according to Eq. 1 [28,32,45].



The morphology, the grain size and the roughness influence the photocatalytic efficiency of TiO<sub>2</sub> films [15,16,35]. Fig. 3 exhibits the AFM image of the undoped and sulfur-doped TiO<sub>2</sub> films. The surface of both the catalysts presents well-defined grains of rounded morphology. Table 2 presents the mean grain size values and RMS (Root Mean Square) roughness. The RMS roughness of the films varied between 10 and 19 nm, values considered favorable for photocatalytic applications, since it facilitates the contact of the adsorbed substances with the film, increasing its photocatalytic efficiency [14,47]. The results presented in Table 2 suggest the influence of the sulfur doping process on the morphological characteristics of TiO<sub>2</sub> films. The mean grain size values were determined by Feret diameter of the particles, in other words, the maximum length of a grain measured in a fixed direction (distance between tangents) [48]. It is noted that the S-TiO<sub>2</sub> film exhibited a reduction of the RMS roughness values and a grain size refinement, compared to the same parameters of the undoped TiO<sub>2</sub> film. This refinement can be attributed to the presence of SO<sub>4</sub><sup>2-</sup> groups on the catalyst surface. Recent papers show that the SO<sub>4</sub><sup>2-</sup> species on S-TiO<sub>2</sub> surface may eventually form two possible coordination models, as proposed for Zhang et al. [25] and Yang et al. [49]. Chen et al. [26] suggested that anatase-TiO<sub>2</sub> surface is very active for H<sub>2</sub>S desulfurization under a H<sub>2</sub> reducing atmosphere, and can facilitate its reaction with the OH<sup>·</sup> superficial. This effect promotes a superficial uniformity of the catalyst, which allows to increase its surface area and consequently its photocatalytic efficiency [14,50,51].

FE-SEM was used to determinate the films thickness from cross-sectional images. Fig. 4 reveals the formation of a dense columnar structure film, characteristic from TiO<sub>2</sub> films grown by MOCVD at 400 °C [10,15,16]. The films grow perpendicular to the substrate surface. In Fig. 4b it can be seen that the films remain homogeneous and preserve the thickness after the sulfur-doping process.

Table 2

Summary of the S doping effect on the morphology characteristics of TiO<sub>2</sub> films grown at 400 °C on borosilicate substrates by MOCVD process.

	Film thickness (nm)	Mean grain size (nm)	RMS roughness (nm)
undoped TiO <sub>2</sub>	351	123	18.9
S-TiO <sub>2</sub>	348	86	10.2

### 3.2. Photocatalytic activity of undoped and sulfur-doped TiO<sub>2</sub> films

The photocatalytic behavior of the undoped and sulfur-doped TiO<sub>2</sub> films on the MO dye degradation under visible light was evaluated, as it can be seen in Fig. 5. The C/C<sub>0</sub> graph exhibits the dye degradation as a function of the time of exposition to source radiation for 300 min, with and without the presence of catalysts. C represents the dye concentration at each time interval and C<sub>0</sub> is the initial concentration. The photolysis curves indicated that without the presence of the catalysts there was no MO dye degradation under visible light, independent of the light intensity. Undoped anatase-TiO<sub>2</sub> film did not present photocatalytic activity under visible light. Other studies showed a similar trend [24,52]. During the photocatalytic experiments, the pH values were constantly monitored. At the start of the tests the pH of dye solution was 2.03. Over the photocatalytic experiments the pH varied slightly around a mean value of 2.35 ± 0.02.

The effect of visible light intensity on photocatalytic activity of films was examined, and the results revealed that the light intensity strongly influences the photocatalytic activity of the films. The S-TiO<sub>2</sub> film exhibited 25% of MO dye degradation under visible light intensity at 30 W for a total test time of 300 min (Fig. 5a), while the same photocatalyst degraded 38% of MO dye under visible light intensity of 240 W (Fig. 5b), that is, it was 52% more efficient. The results reached are in line with the values obtained by AFM, which confirms the influence of grain size and roughness on the photodegradation efficiency of the films. Smaller grain sizes provide the increasing of the TiO<sub>2</sub> specific surface area [39,53]. A larger surface area allows greater contact of the photocatalyst with the pollutant compound and with the light irradiation which consequently favors the photocatalytic efficiency [24].

SO<sub>4</sub><sup>2-</sup> groups present on the surface of the sulfur-doped film represent a highly photoactivated morphology. The substitution of the Ti<sup>4+</sup> by S<sup>6+</sup> ions promotes the formation of Ti-O-S bonds, which allows to modify the electronic structure of TiO<sub>2</sub> by displacing the electronic sites from O to S [14,42,54], as suggested in Fig. 6. The oxygen atom becomes a deficient center that hinders the recombination of the electron-hole pairs under visible light [25]. Yan et al [44] suggest that the band gap narrowing of the S-doped TiO<sub>2</sub> catalysts can be ascribed to Pauling electronegativity concept, where the sulfur electronegativity (2.58) is lower than oxygen (3.44), which is beneficial to location of the S 3p atomic orbital at higher energies than the O 2p atomic orbital. In this way, the narrowing band gap by intermediate energy states formation into S-TiO<sub>2</sub> can stimulate the generation of electron (e<sup>-</sup>)/hole (h<sup>+</sup>) pairs, and possibly increase the production of OH<sup>·</sup> species under visible light irradiation, which is a decisive catalytic step for efficient water treatment and environment applications.

It was possible to observe that the visible light intensity influences the photocatalytic activity of sulfur-doped films. The reduction of the

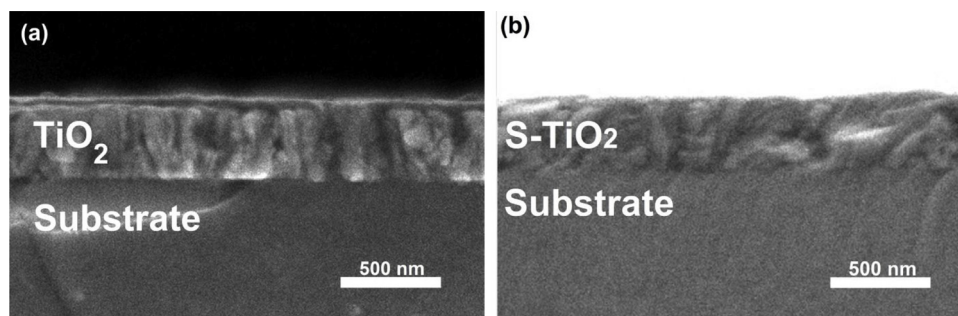


Fig. 4. Cross-sectional FE-SEM images of (a) undoped TiO<sub>2</sub> film grown at 400 °C on borosilicate substrate by MOCVD; and (b) sulfur-doped TiO<sub>2</sub> film.

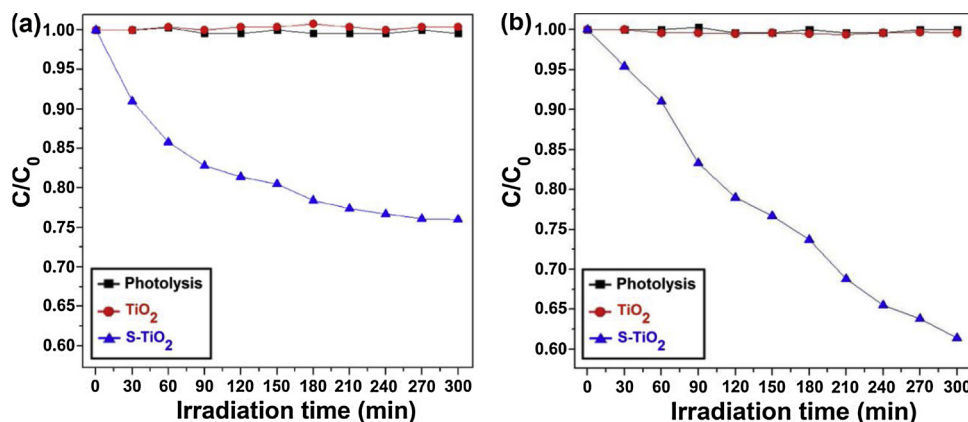


Fig. 5. Methyl orange dye degradation as a function of the time of exposure to visible light with and without the presence of undoped and sulfur-doped TiO<sub>2</sub> films grown by MOCVD at 400 °C: (a) visible light with luminous intensity at 30 W; (b) visible light with luminous intensity at 240 W.

luminous intensity caused a restriction on the photocatalytic efficiency of the films, due to the reduction of the number of photons emitted to the solution and on the semiconductor surface, thus reducing the number of activated catalyst particles, and producing less hydroxyl radicals [55]. According to kinetic studies of photocatalytic reactions, the degradation rate increases with increasing the light intensity in a non-linear relationship [56]. Similar conclusion has been reported by previous studies employing other types of catalysts and dopants [55,57,58]. It is noted that the MO dye degradation slows down after 120 min irradiation for S-TiO<sub>2</sub> catalyst. Wang et al. [24] suggest that this effect is caused by the adsorbates induced by the initial fast degradation and may prevent further reaction. The results indicated that the sulfur doping can significantly improve the photocatalytic activity of the TiO<sub>2</sub> and leads to absorption of visible light irradiation. The results support the idea that the sulfur-doped TiO<sub>2</sub> films grown by MOCVD may be promising catalysts for the water treatment.

#### 4. Conclusions

The present research showed the study of the photocatalytic activity and the structural and morphological characteristics of undoped and sulfur-doped TiO<sub>2</sub> films grown at 400 °C on borosilicate substrates by MOCVD process. The sulfur doping was realized at 50 °C by a process similar to that used for the desulfurization of H<sub>2</sub>S in gas-phase. The films presented the formation of anatase phase, surface morphology composed of rounded grains, and a dense columnar structure. Without the presence of the catalyst, there was no dye degradation. Undoped TiO<sub>2</sub> film did not present photocatalytic activity under visible light. S-TiO<sub>2</sub> film exhibited good photocatalytic activity under visible light irradiation on methyl orange dye degradation. The results reveal that the light intensity strongly influences the photocatalytic behavior of S-TiO<sub>2</sub> films. The best photocatalytic result occurred for the S-TiO<sub>2</sub> film under visible light with intensity at 240 W, that exhibited 38% of dye

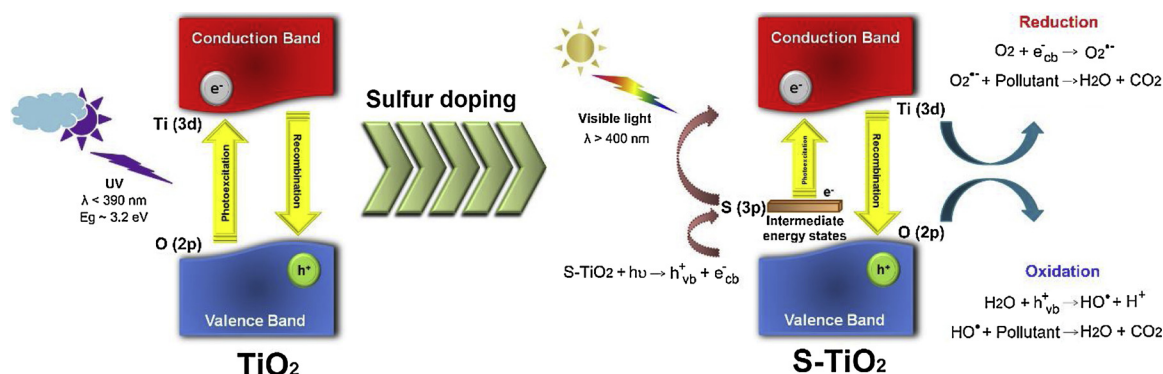


Fig. 6. Schematic illustration of the sulfur doping process effect on narrowing the band gap of TiO<sub>2</sub> catalyst, where it is possible to observe the formation of the localized intermediate energy states for the substitutionally S-doped TiO<sub>2</sub> and its mechanism of semiconductor heterogeneous photocatalysis, respectively.

degradation – 52% more efficient than under visible light at 30 W. An increase in the light intensity accelerated the degradation rate due to the increase of the number of photons that reaches the semiconductor surface. Sulfur doping at 50 °C in H<sub>2</sub>/H<sub>2</sub>S atmosphere can significantly improve the photocatalytic activity of the TiO<sub>2</sub> under visible light, which allows their practical application under sunlight or visible light bulbs. The results supported the idea that the sulfur-doped TiO<sub>2</sub> films grown by MOCVD may be promising catalysts for water treatment by a green method.

### Conflicts of interest

The authors declare no conflict of interest.

### Acknowledgments

The authors would like to thank CAPES (Coordination for the Improvement of Higher Education Personnel) for the financial support, and UFABC (Federal University of ABC) for the XPS facility.

### References

- [1] K.M. Reza, A.S.W. Kurny, F. Gulshan, Parameters affecting the photocatalytic degradation of dyes using TiO<sub>2</sub>: a review, *Appl. Water Sci.* 7 (2017) 1569–1578, <https://doi.org/10.1007/s13201-015-0367-y>.
- [2] F.M.D. Chequer, G.A.R. Oliveira, E.R.A. Ferraz, J.C. Cardoso, M.V.B. Zanoni, D.P. Oliveira, Textile dyes: dyeing process and environmental impact, in: M. Gunay (Ed.), *Eco-Friendly Textile Dyeing and Finishing*, InTech, Rijeka, 2013, pp. 151–176, <https://doi.org/10.5772/53659>.
- [3] R. Guz, C. Moura, M.A.A. Cunha, Factorial design application in photocatalytic wastewater degradation from TNT industry-red water, *Environ. Sci. Pollut. Res. Int.* 24 (2017) 6055–6060, <https://doi.org/10.1007/s11356-016-6460-4>.
- [4] D. Hermosilla, N. Merayo, A. Gascó, Á. Blanco, The application of advanced oxidation technologies to the treatment of effluents from the pulp and paper industry: a review, *Environ. Sci. Pollut. Res.* 22 (2015) 168–191, <https://doi.org/10.1007/s11356-014-3516-1>.
- [5] O. Sacco, V. Vaiano, L. Rizzo, D. Sannino, Photocatalytic activity of a visible light active structured photocatalyst developed for municipal wastewater treatment, *J. Clean. Produc.* 175 (2018) 38–49, <https://doi.org/10.1016/j.jclepro.2017.11.088>.
- [6] M. Horáková, S. Klementová, P. Kriz, S.K. Balakrishna, P. Spatenka, O. Golovko, P. Hájková, P. Exnar, The synergistic effect of advanced oxidation processes to eliminate resistant chemical compounds, *Surf. Coat. Technol.* 24 (2014) 154–158, <https://doi.org/10.1016/j.surfcoat.2013.10.068>.
- [7] S. Shin, H. Yoon, J. Jang, Polymer-encapsulated iron oxide nanoparticles as highly efficient Fenton catalysts, *Catal. Commun.* 10 (2008) 178–182, <https://doi.org/10.1016/j.catcom.2008.08.027>.
- [8] S. Tsoumachidou, D. Lambropoulou, I. Poullos, Homogeneous photocatalytic oxidation of UV filter para-amino benzoic acid in aqueous solutions, *Environ. Sci. Pollut. Res.* 24 (2017) 1113–1121, <https://doi.org/10.1007/s11356-016-7434-2>.
- [9] J. Ângelo, P. Magalhães, L. Andrade, A. Mendes, Characterization of TiO<sub>2</sub>-based semiconductors for photocatalysis by electrochemical impedance spectroscopy, *Appl. Surf. Sci.* 387 (2016) 183–189, <https://doi.org/10.1016/j.apsusc.2016.06.101>.
- [10] R.T. Bento, A. Ferrus Filho, M.F. Pillis, Microstructural characterization of TiO<sub>2</sub> thin films: a review, *Rev. Bras. Inov. Tecnol. Em Saúde* 7 (2017) 4–17, <https://doi.org/10.18816/r-bits.v7i2>.
- [11] Y. Cao, Z. Fu, W. Wei, L. Zou, T. Mi, D. He, C. Yan, X. Liu, Y. Zhu, L. Chen, Y. Sun, Reduced graphene oxide supported titanium dioxide nanomaterials for the photocatalysis with long cycling life, *Appl. Surf. Sci.* 355 (2015) 1289–1294, <https://doi.org/10.1016/j.apsusc.2015.08.036>.
- [12] S. Athalathil, B. Erjavec, R. Kaplan, F. Stuber, C. Bengoa, J. Font, A. Fortuny, A. Pintar, A. Fabregat, TiO<sub>2</sub>-sludge carbon enhanced catalytic oxidative reaction in environmental wastewaters applications, *J. Hazard. Mater.* 300 (2015) 406–414, <https://doi.org/10.1016/j.jhazmat.2015.07.025>.
- [13] S.M. El-Sheikh, T.M. Khedra, A. Hakkib, A.A. Ismaila, W.A. Badawy, D.W. Bahnemann, Visible light activated carbon and nitrogen co-doped mesoporous TiO<sub>2</sub> as efficient photocatalyst for degradation of ibuprofen, *Sep. Purif. Technol.* 173 (2017) 258–268, <https://doi.org/10.1016/j.seppur.2016.09.034>.
- [14] R.T. Bento, Study of the Photocatalytic Activity of Sulfur-doped TiO<sub>2</sub> Films. Master Dissertation, Nuclear and Energy Research Institute, University of São Paulo, 2018 113 pp..
- [15] A.J. Gardecka, C. Bishop, D. Lee, S. Corby, I.P. Parkin, A. Kafizas, S. Krumdieck, High efficiency water splitting photoanodes composed of nanostructured anatase-rutile TiO<sub>2</sub> heterojunctions by pulsed-pressure MOCVD, *Appl. Catal. B: Environ.* 224 (2018) 904–911, <https://doi.org/10.1016/j.apcatb.2017.11.033>.
- [16] B.A. Marcello, Microstructural, Morphologic and Photocatalytic Characterization of TiO<sub>2</sub> Thin Films Grown by Metalorganic Chemical Vapor Deposition. Master Dissertation, Nuclear and Energy Research Institute, University of São Paulo, 2015 97 pp..
- [17] M. Dhayal, R. Kapoor, P.G. Sistla, R.R. Pandey, S. Kar, K.K. Saini, G. Pande, Strategies to prepare TiO<sub>2</sub> thin films, doped with transition metal ions, that exhibit specific physicochemical properties to support osteoblast cell adhesion and proliferation, *Mater. Sci. Eng. C Mater. Biol. Appl.* 37 (2014) 99–107, <https://doi.org/10.1016/j.msec.2013.12.035>.
- [18] D.A.H. Hanaor, C.C. Sorrell, Review of the anatase to rutile phase transformation, *J. Mater. Sci.* 46 (2011) 855–874, <https://doi.org/10.1007/s10853-010-5113-0>.
- [19] K.A. Borges, L.M. Santos, R.M. Paniago, N.M.B. Neto, J. Schneider, D.W. Bahnemann, A.O.T. Patrocínio, A.E.H. Machado, Characterization of a highly efficient N-doped TiO<sub>2</sub> photocatalyst prepared via factorial design, *New J. Chem.* 40 (2016) 7846–7855, <https://doi.org/10.1039/c6nj00704j>.
- [20] D. Duc La, A. Rananaware, H.P. NguyenThi, L. Jones, S.V. Bhosale, Fabrication of a TiO<sub>2</sub>@porphyrin nanofiber hybrid material: a highly efficient photocatalyst under simulated sunlight irradiation, *Adv. Nat. Sci: Nanosci. Nanotechnol.* 8 (2017) 015009, <https://doi.org/10.1088/2043-6254/aa597e>.
- [21] M.R. Bayati, A.Z. Moshfegh, F. Golestani-Fard, On the photocatalytic activity of the sulfur doped titanium nano-porous films derived via micro-arc oxidation, *Appl. Catal. A, Gen.* 389 (2010) 60–67, <https://doi.org/10.1016/j.apcata.2010.09.003>.
- [22] T. Ohno, M. Akiyoshi, T. Umebayashi, K. Asai, T. Mitsui, M. Matsumura, Preparation of S-doped TiO<sub>2</sub> photocatalysts and their photocatalytic activities under visible light, *Appl. Catal. A-Gen.* 265 (2004) 115–121, <https://doi.org/10.1016/j.apcata.2004.01.007>.
- [23] C. Han, M. Pelaez, V. Likodimos, A.G. Kontos, P. Falaras, K. O’Shea, D.D. Dionysiou, Innovative visible light-activated sulfur doped TiO<sub>2</sub> films for water treatment, *Appl. Catal. B: Environ.* 107 (2011) 77–87, <https://doi.org/10.1016/j.apcatb.2011.06.039>.
- [24] F. Wang, F. Li, L. Zhang, H. Zeng, Y. Sun, S. Zhang, X. Xu, S-TiO<sub>2</sub> with enhanced visible-light photocatalytic activity derived from TiS<sub>2</sub> in deionized water, *Mater. Res. Bull.* 87 (2017) 20–26, <https://doi.org/10.1016/j.materresbull.2016.11.014>.
- [25] F. Zhang, M. Wang, X. Zhu, B. Hong, W. Wang, Z. Qi, W. Xie, J. Ding, J. Bao, S. Sun, C. Gao, Effect of surface modification with H<sub>2</sub>S and NH<sub>3</sub> on TiO<sub>2</sub> for adsorption and photocatalytic degradation of gaseous toluene, *Appl. Catal. B: Environ.* 170–171 (2015) 215–224, <https://doi.org/10.1016/j.apcatb.2015.01.045>.
- [26] Y. Chen, Y. Jiang, W. Li, R. Jin, S. Tang, W. Hu, Adsorption and interaction of H<sub>2</sub>S/SO<sub>2</sub> on TiO<sub>2</sub>, *Catal. Today* 50 (1999) 39–47, [https://doi.org/10.1016/S0920-5861\(98\)00460-X](https://doi.org/10.1016/S0920-5861(98)00460-X).
- [27] S. Cravanzola, F. Cesano, F. Gaziano, D. Scarano, Sulfur-doped TiO<sub>2</sub>: structure and surface properties, *Catalysts* 7 (2017), <https://doi.org/10.3390/catal707214> 214 (11pp.).
- [28] M.C. Canela, R.M. Alberici, W.F. Jardim, Gas-phase destruction of H<sub>2</sub>S using TiO<sub>2</sub>/UV-VIS, *J. Photochem. Photobiol. A: Chem.* 112 (1998) 73–80, [https://doi.org/10.1016/S1010-6030\(97\)00261-X](https://doi.org/10.1016/S1010-6030(97)00261-X).
- [29] R. Portela, B. Sánchez, J.M. Coronado, Photocatalytic oxidation of H<sub>2</sub>S on TiO<sub>2</sub> and TiO<sub>2</sub>-ZrO<sub>2</sub> thin films, *J. Adv. Oxid. Technol.* 10 (2) (2007) 375–380, <https://doi.org/10.1515/jaots-2007-0223>.
- [30] C. Liu, R. Zhang, S. Wei, J. Wang, Y. Liu, M. Li, R. Liu, Selective removal of H<sub>2</sub>S from biogas using a regenerable hybrid TiO<sub>2</sub>/zeolite composite, *Fuel* 157 (2015) 183–190, <https://doi.org/10.1016/j.fuel.2015.05.003>.
- [31] A. Jurekaew, P. Maitarad, R. Arryave, N. Kungwan, D. Zhang, L. Shi, S. Namsuangruk, The complete reaction mechanism of H<sub>2</sub>S desulfurization on an anatase TiO<sub>2</sub> (001) surface: a density functional theory investigation, *Catal. Sci. Technol.* 7 (2) (2017) 356–365, <https://doi.org/10.1039/c6cy02030e>.
- [32] A. Alonso-Tellez, D. Robert, N. Keller, V. Keller, A parametric study of the UV-A photocatalytic oxidation of H<sub>2</sub>S over TiO<sub>2</sub>, *Appl. Catal. B: Environ.* 115–116 (2012) 209–218, <https://doi.org/10.1016/j.apcatb.2011.12.014>.
- [33] M. Li, Z. Xing, J. Jiang, Z. Li, J. Kuang, J. Yin, N. Wan, Q. Zhu, W. Zhou, In-situ Ti<sup>3+</sup>/S doped high thermostable anatase TiO<sub>2</sub> nanorods as efficient visible-light-driven photocatalysts, *Mater. Chem. Phys.* 219 (2018) 303–310, <https://doi.org/10.1016/j.matchemphys.2018.08.051>.
- [34] J. Walton, P. Wincott, N. Fairley, A. Carrick, *Peak Fitting With CasaXPS, A Casa Pocket Book*, (2010).
- [35] R.T. Bento, M.F. Pillis, Titanium dioxide films for photocatalytic degradation of methyl Orange dye, *Titanium Dioxide - Material for a Sustainable Environment*, 1 ed., InTech, London, 2018, pp. 211–226, <https://doi.org/10.5772/intechopen.75528>.
- [36] H. Seo, S.H. Nam, N. Itagaki, K. Koga, M. Shiratani, J.H. Boo, Effect of sulfur doped TiO<sub>2</sub> on photovoltaic properties of dye-sensitized solar cells, *Electron. Mater. Lett.* 12 (2016) 530–536, <https://doi.org/10.1007/s13391-016-4018-8>.
- [37] R. Liu, X. Zhou, F. Yang, Y. Yu, Combination study of DFT calculation and experiment for photocatalytic properties of S-doped anatase TiO<sub>2</sub>, *Appl. Surf. Sci.* 319 (2014) 50–59, <https://doi.org/10.1016/j.apsusc.2014.07.132>.
- [38] P. Babelon, A.S. Dequiedt, H. Mostéfa-Sba, S. Bourgeois, P. Sibillot, M. Sacilott, SEM and XPS studies of titanium dioxide thin films grown by MOCVD, *Thin Solid Films* 332 (1998) 63–67, [https://doi.org/10.1016/S0040-6090\(97\)00958-9](https://doi.org/10.1016/S0040-6090(97)00958-9).
- [39] B. Anitha, C. Ravidhas, R. Venkatesh, A.M.E. Raj, K. Ravichandran, B. Subramanian, C. Sanjeeviraja, Self assembled sulfur induced interconnected nanostructure TiO<sub>2</sub> electrode for visible light photoresponse and photocatalytic application, *Phys. E: Low-Dimensional Syst. Nanostruct.* 91 (2017) 148–160, <https://doi.org/10.1016/j.physe.2017.04.017>.
- [40] P. Georgios, S.M. Wolfgang, X-ray photoelectron spectroscopy of anatase-TiO<sub>2</sub> coated carbon nanotubes, *Solid State Phenom.* 162 (2010) 163–177, <https://doi.org/10.4028/www.scientific.net/SSP.162.163>.
- [41] W. Zhao, X. Feng, H. Xiao, C. Luan, J. Ma, Structural and optical properties of anatase TiO<sub>2</sub> heteroepitaxial films prepared by MOCVD, *J. Korean Cryst. Growth Cryst. Technol.* 453 (2016) 106–110, <https://doi.org/10.1016/j.jcrysgro.2016.08.020>.

- [42] L.G. Devi, R. Kavitha, Enhanced photocatalytic activity of sulfur doped TiO<sub>2</sub> for the decomposition of phenol: a new insight into the bulk and surface modification, *Mater. Chem. Phys.* 143 (2014) 1300–1309, <https://doi.org/10.1016/j.matchemphys.2013.11.038>.
- [43] N. Yao, C. Wu, L. Jia, S. Han, B. Chi, J. Pu, L. Jian, Simple synthesis and characterization of mesoporous (N, S)-codoped TiO<sub>2</sub> with enhanced visible-light photocatalytic activity, *Ceram. Int.* 38 (2012) 1671–1675, <https://doi.org/10.1016/j.ceramint.2011.09.059>.
- [44] X. Yan, K. Yuan, N. Lu, H. Xu, S. Zhang, N. Takeuchi, H. Kobayashi, R. Li, The interplay of sulfur doping and surface hydroxyl in band gap engineering: mesoporous sulfur-doped TiO<sub>2</sub> coupled with magnetite as a recyclable, efficient, visible light active photocatalyst for water purification, *Appl. Catal. B: Environ.* 218 (2017) 20–31, <https://doi.org/10.1016/j.apcatb.2017.06.022>.
- [45] N. Shahzad, S.T. Hussain, A. Siddiqua, M.A. Baig, A comparison of TiO<sub>2</sub> nanoparticles and nanotubes for catalytic gas phase destruction of H<sub>2</sub>S gas at high temperatures, *J. Nanosci. Nanotechnol.* 12 (6) (2012) 5061–5065, <https://doi.org/10.1166/jnn.2012.4934>.
- [46] C.S.W. Jeffrey, Photocatalytic reduction of greenhouse gas CO<sub>2</sub> to fuel, *Catal. Surv. Asia* 13 (2009) 30–40, <https://doi.org/10.1007/s10563-009-9065-9>.
- [47] O. Carp, C.L. Huisman, A. Reller, Photoinduced reactivity of titanium dioxide, *Prog. Solid State Chem.* 32 (2004) 33–177, <https://doi.org/10.1016/j.progsolidstchem.2004.08.001>.
- [48] B.H. Kaye, *Particle Image Analysis, ASM Handbook*, (1998), pp. 259–273.
- [49] G. Yang, Z. Yan, T. Xiao, Low-temperature solvothermal synthesis of visible-light-responsive S-doped TiO<sub>2</sub> nanocrystal, *Appl. Surf. Sci.* 258 (2012) 4016–4022, <https://doi.org/10.1016/j.apsusc.2011.12.092>.
- [50] X.L. Peng, M.M. Yao, F. Li, X.H. Sun, Microstructures and photocatalytic properties of S doped nanocrystalline TiO<sub>2</sub> films, *Particul. Sci. Technol.* 30 (2012) 81–91, <https://doi.org/10.1080/02726351.2010.551711>.
- [51] I. Oja Acik, V. Kiisk, M. Krunks, I. Sildos, A. Junolainen, M. Danilson, A. Mere, V. Mikli, Characterization of samarium and nitrogen co-doped TiO<sub>2</sub> films prepared by chemical spray pyrolysis, *Appl. Surf. Sci.* 261 (2012) 735–741, <https://doi.org/10.1016/j.apsusc.2012.08.090>.
- [52] C.W. Dunnill, Z.A. Aiken, A. Kafizas, J. Pratten, M. Wilson, D.J. Morgan, I.P. Parkin, White light induced photocatalytic activity of sulfur-doped TiO<sub>2</sub> thin films and their potential for antibacterial application, *J. Mater. Chem.* 19 (2009) 8747–8754, <https://doi.org/10.1039/b913793a>.
- [53] C.S. Park, U.K.H. Bangi, H.H. Park, Effect of sulfur dopants on the porous structure and electrical properties of mesoporous TiO<sub>2</sub> thin films, *Mater. Lett.* 106 (2013) 401–404, <https://doi.org/10.1016/j.matlet.2013.05.091>.
- [54] W.F. Huang, H.T. Chen, M.C. Lin, Density functional theory study of the adsorption and reaction of H<sub>2</sub>S on TiO<sub>2</sub> rutile (110) and anatase (101) surfaces, *J. Phys. Chem. C* 113 (2009) 20411–20420, <https://doi.org/10.1021/jp906948a>.
- [55] H.M. Hadi, H.S. Wahab, Visible light photocatalytic decolourization of methyl orange using N-doped TiO<sub>2</sub> nanoparticles, *J. Al-Nahrain Univ.* 18 (2015) 1–9.
- [56] S. Munesh, R.C. Meena, Photocatalytic degradation of textile dye through an alternative photocatalyst methylene blue immobilized resin dowex 11 in presence of solar light, *Arch. Appl. Sci. Res.* 4 (2012) 472–479.
- [57] P.B. Punjabi, R. Ameta, A. Kumar, M. Jain, Visible light induced photocatalytic degradation of some xanthene dyes using immobilized anthracene, *Bull. Chem. Soc. Ethiop.* 22 (2008) 361–368, <https://doi.org/10.4314/bcse.v22i3.61208>.
- [58] V.S. Slusarski, A.L. Alberton, N.R.G. Machado, Influence of luminous intensity on textile effluent photodegradation, *Acta Sci. Pol. Technol. Aliment.* 27 (2005) 1–6.